

Bulk viscosity and contact correlations in attractive Fermi gases

Tilman Enss

Institut für Theoretische Physik, Universität Heidelberg, D-69120 Heidelberg, Germany

(Dated: January 26, 2022)

The bulk viscosity determines dissipation during hydrodynamic expansion. It vanishes in scale invariant fluids, while a nonzero value quantifies the deviation from scale invariance. For the dilute Fermi gas the bulk viscosity is given exactly by the correlation function of the contact density of local pairs. As a consequence, scale invariance is broken purely by pair fluctuations. These fluctuations give rise also to logarithmic terms in the bulk viscosity of the high-temperature nondegenerate gas. For the quantum degenerate regime I report numerical Luttinger-Ward results for the contact correlator and the dynamical bulk viscosity throughout the BEC-BCS crossover. The ratio of bulk to shear viscosity ζ/η is found to exceed the kinetic theory prediction in the quantum degenerate regime. Near the superfluid phase transition the bulk viscosity is enhanced by critical fluctuations and has observable effects on dissipative heating, expansion dynamics and sound attenuation.

The bulk viscosity is a fundamental transport property which determines friction and dissipation in fluids during hydrodynamic expansion [1, 2]. In particular, scale invariant fluids can expand isotropically without dissipation and therefore have zero bulk viscosity [3]. In a generic interacting fluid, instead, a nonzero value of the bulk viscosity quantifies the breaking of scale invariance in physical systems ranging from QCD [4–7] to condensed matter [8–14]. An intriguing example is the two-dimensional dilute Fermi gas, where the classical model is scale invariant but a quantum scale anomaly breaks this symmetry [15–18]; this has recently been observed via breathing dynamics in cold-atom experiments [19–21].

The bulk viscosity is necessary to understand and predict the real-time evolution and hydrodynamic modes of dissipative quantum fluids and to quantitatively interpret current experiments. However, measurements of the bulk viscosity remain challenging even for classical fluids [22]. Now a novel experimental probe via the dissipative heating rate due to a change in scattering length has been proposed for atomic gases [14]. It is therefore important to compute the bulk viscosity theoretically for quantum gases, which moreover includes predictions for the classical gas in the high-temperature limit.

The bulk viscosity is defined as the correlation function of local pressure (the trace of the stress tensor). Since it vanishes in a scale invariant system, only the scale breaking part of the pressure contributes, the so-called trace anomaly [14, 23, 24]. This provides a formal link between the breaking of scale invariance and bulk viscosity. The bulk viscosity of the nonrelativistic, strongly interacting Fermi gas has been calculated from kinetic theory in the nondegenerate high-temperature limit [11, 12] and in the low-temperature superfluid state [25, 26]. Its value is largest in the strongly coupled region of the BEC-BCS crossover [27] near unitarity, but not precisely at unitarity where it must vanish by scale invariance [3, 9, 28]. Furthermore, hydrodynamic fluctuations give rise to non-analytic corrections to the bulk viscosity at small frequencies [23, 29]. However, key open questions include

the bulk viscosity in degenerate Fermi gases at strong interaction, the relative importance of bulk and shear viscosity, and critical scaling near the superfluid phase transition.

In this work, I rewrite the bulk viscosity of the dilute Fermi gas as a correlation function of the contact density of local fermion pairs. This exact mapping explicitly links the bulk viscosity to pairing fluctuations as the relevant degrees of freedom and provides a genuine strong-coupling formulation which is valid in the whole BEC-BCS crossover including the quantum critical regime [30–32]. New results include (a) dominant logarithmic corrections to the bulk viscosity at high temperature, (b) numerical Luttinger-Ward results for the quantum degenerate gas throughout the BEC-BCS crossover predict a large bulk viscosity well observable with current experimental technology, (c) the transport ratio of bulk to shear viscosity deviates from the kinetic theory prediction in the quantum degenerate regime, and (d) critical scaling near the superfluid transition is less singular than predicted [29, 33], but pairing fluctuations dynamically enhance the scale anomaly.

Bulk viscosity.—The bulk viscosity ζ is defined as the stress correlation function [8, 34, 35]

$$\zeta(\omega) = -\frac{1}{\omega d^2} \text{Im} \int_0^\infty dt e^{i\omega t} \int d^d x \langle [\hat{\Pi}_{ii}(\mathbf{x}, t), \hat{\Pi}_{jj}(0, 0)] \rangle, \quad (1)$$

where the trace of the stress tensor $\hat{\Pi}_{ii}(\mathbf{x}, t) = d \cdot \hat{P}$ determines the pressure operator \hat{P} in dimension d . The two-component dilute Fermi gas is described by the Hamiltonian density [27]

$$\hat{\mathcal{H}} = \sum_{\sigma} \psi_{\sigma}^{\dagger} \left(-\frac{\nabla^2}{2m} \right) \psi_{\sigma} + g_0 \psi_{\uparrow}^{\dagger} \psi_{\downarrow}^{\dagger} \psi_{\downarrow} \psi_{\uparrow}. \quad (2)$$

The first term denotes the kinetic energy with fermion operators $\psi_{\sigma}(\mathbf{x}, t)$. The attractive contact interaction in the second term is characterized by the s -wave scattering length a . For a given value of a , the bare coupling strength g_0 is determined according to $g_0^{-1} =$

$-(m/2\pi)\ln(a\Lambda)$ in two dimensions (2D) and $g_0^{-1} = (m/4\pi)(1/a - 2\Lambda/\pi)$ in 3D, with ultraviolet momentum cutoff Λ . The trace of the stress tensor is given by the scale variation of the Hamiltonian [17],

$$d \cdot \hat{P} = \hat{\Pi}_{ii} = [\hat{\mathcal{H}}, i\hat{D}] = 2\hat{\mathcal{H}} + \begin{cases} \frac{\hat{\mathcal{C}}}{2\pi m} & (2D), \\ \frac{\hat{\mathcal{C}}}{4\pi m a} & (3D), \end{cases} \quad (3)$$

where the dilatation operator $\hat{D} = \int d^d x \mathbf{x} \cdot m \mathbf{j}(\mathbf{x})$ generates scale transformations. The first term on the right-hand side is the scale invariant result $[\hat{\mathcal{H}}, i\hat{D}] = 2\hat{\mathcal{H}}$. If only this is present, the pressure is proportional to the Hamiltonian and commutes with itself in (1), hence the bulk viscosity $\zeta(\omega) \equiv 0$ vanishes identically in the scale invariant case [3, 9, 28, 36].

The second term, in turn, is proportional to the local pair contact density $\hat{\mathcal{C}} = -m^2(\partial\hat{\mathcal{H}}/\partial g_0^{-1}) = m^2 g_0^2 \psi_\uparrow^\dagger \psi_\downarrow^\dagger \psi_\downarrow \psi_\uparrow$ [37]. Scale invariance is recovered for the ideal quantum gas where $\hat{\mathcal{C}} = 0$, and also for the 3D unitary Fermi gas where $1/a = 0$ at the scattering resonance. A nonzero bulk viscosity therefore quantifies the breaking of scale invariance, which is generally expected in the interacting Fermi gas, except at unitarity.

Contact correlation.—By conservation of energy, the Hamiltonian in (3) does not contribute to the pressure commutator (1), and the bulk viscosity is given by the correlator of the scale breaking term. The scaling violation in the trace of the stress tensor is the so-called trace anomaly [14, 23]

$$\hat{\Pi}_{\text{an}} \equiv \hat{\Pi}_{ii} - 2\hat{\mathcal{H}} = c_d \hat{\mathcal{C}}, \quad (4)$$

where $c_d = -(\partial g_0^{-1}/\partial \ln|a|)/m^2$ denotes the scale variation of the bare coupling (beta function). For the dilute gas, the equilibrium bulk viscosity is thus exactly given by the contact correlator,

$$\zeta(\omega) = -\frac{c_d^2}{\omega d^2} \text{Im} \int_0^\infty dt e^{i\omega t} \int d^d x \langle [\hat{\mathcal{C}}(\mathbf{x}, t), \hat{\mathcal{C}}(0, 0)] \rangle. \quad (5)$$

The contact operator is the term in the Hamiltonian which couples to the scattering length. In linear response, the bulk viscosity thus captures how the local pair contact density at time t changes in response to a variation of the scattering length at earlier time $t = 0$ [14],

$$\chi(\mathbf{x}, t) \equiv \langle [\hat{\mathcal{C}}(\mathbf{x}, t), \hat{\mathcal{C}}(0, 0)] \rangle = \begin{cases} 2\pi m \left(\frac{\partial \langle \hat{\mathcal{C}}(\mathbf{x}, t) \rangle}{\partial \ln a(0, 0)} \right)_s & (2D), \\ -4\pi m \left(\frac{\partial \langle \hat{\mathcal{C}}(\mathbf{x}, t) \rangle}{\partial a^{-1}(0, 0)} \right)_s & (3D) \end{cases} \quad (6)$$

at constant entropy per particle $s = S/N$. The time dependent contact response captures how quickly the contact adjusts to a change in scattering length; this directly determines the dynamical bulk viscosity according to Eq. (5). This makes the contact correlation, and

hence the dynamical bulk viscosity, directly accessible in cold atom experiments where the scattering length can be controlled in time by the magnetic field near a Feshbach resonance and the time evolution of the contact has already been measured using RF spectroscopy [38, 39].

Viscosity sum rule.—Since the pressure operator is hermitean, the dynamical bulk viscosity is an even and positive function of frequency, $\zeta(\omega) \geq 0$ [8]. The integral over all frequencies in Eqs. (5), (6) immediately yields the bulk viscosity sum rule [8, 10] with $\mathcal{C} = \langle \hat{\mathcal{C}} \rangle$,

$$S \equiv \frac{2}{\pi} \int_0^\infty d\omega \zeta(\omega) = \begin{cases} -\frac{1}{8\pi m} \left(\frac{\partial \mathcal{C}}{\partial \ln a} \right)_s & (2D), \\ \frac{1}{36\pi m a^2} \left(\frac{\partial \mathcal{C}}{\partial a^{-1}} \right)_s & (3D). \end{cases} \quad (7)$$

Using the Tan adiabatic relation to express the contact $\Pi_{\text{an}} = c_d \mathcal{C} = (\partial \mathcal{E}/\partial \ln|a|)_s$ as the scale variation of the energy density \mathcal{E} [17, 37, 40], the sum rule is given by the scale “susceptibility” $S = -(1/d^2)(\partial^2 \mathcal{E}/\partial (\ln|a|)^2)_s \geq 0$ in d dimensions. The sum rule is taken at constant entropy per particle to ensure that the bulk viscosity of the ideal gas is zero [8].

Pair fluctuations.—The local contact density can equivalently be interpreted as the density operator $\hat{\mathcal{C}} = \hat{\Delta}^\dagger \hat{\Delta}(\mathbf{x})$ of the local fermion pair field $\hat{\Delta}(\mathbf{x}) = m g_0 \psi_\downarrow(\mathbf{x}) \psi_\uparrow(\mathbf{x})$. The bulk viscosity thus depends directly, and only, on pairing fluctuations within the attractive Fermi gas; it is given exactly by the four-point pair correlation function $\chi(\mathbf{x}, t) = \langle [\hat{\Delta}^\dagger \hat{\Delta}(\mathbf{x}, t), \hat{\Delta}^\dagger \hat{\Delta}(0, 0)] \rangle$. One can anticipate that the bulk viscosity has a strong signature at the superfluid phase transition which is driven by pair fluctuations (see below). While pair fluctuations are strong also at unitarity, the prefactor $c_d^2 \sim 1/a^2$ ensures that ζ vanishes in this case.

To summarize, the bulk viscosity is the response function of the trace anomaly and is therefore sensitive to scaling violation. For the dilute quantum gas, the trace anomaly is proportional to the contact density of local pairs and depends only on the pairing properties. This establishes the link between pairing [41] and the quantum scale anomaly [21] suggested by recent experiments in 2D Fermi gases.

Analytical results.—The contact correlations and bulk viscosity can be computed exactly in several limiting cases: at (i) zero density (two-body), (ii) high frequency, and (iii) high temperature (virial expansion).

The zero-density case (i) is determined solely by two-body physics. In this limit, the only source of dissipation is the dissociation of a bound molecule at the two-body binding energy $\varepsilon_B = \hbar^2/m a^2$; this yields a high-frequency tail above the threshold $\omega > \varepsilon_B$ to break a pair [10, 42],

$$\zeta_{2D, \text{vac}}(\omega) = \frac{\mathcal{C}_0}{4m\omega} \frac{\Theta(\omega - \varepsilon_B)}{\ln^2(\omega/\varepsilon_B - 1) + \pi^2} \quad (8)$$

in 2D, where \mathcal{C}_0 denotes the two-body contact. In 3D, a two-body bound state exists only on the BEC side for

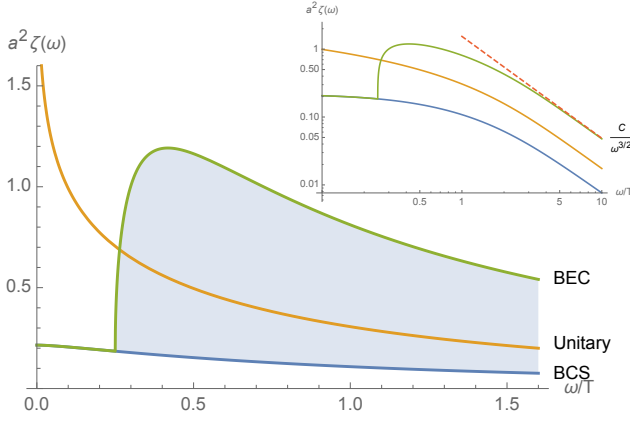


FIG. 1. Dynamical bulk viscosity $\zeta(\omega)/[\sqrt{2}z^2/9\pi a^2\lambda]$ vs frequency ω in the high-temperature limit (11). From top to bottom: BEC ($v = 0.5$, green), Unitary ($v = 0$, orange), BCS ($v = -0.5$, blue). Inset: logarithmic plot shows exact high-frequency asymptotics (10) proportional to $C/\omega^{3/2}$ (dashed).

$a > 0$, and

$$\zeta_{3D,vac}(\omega) = \frac{C_0}{36\pi m a} \frac{\Theta(a) \sqrt{\varepsilon_B(\omega - \varepsilon_B)} \Theta(\omega - \varepsilon_B)}{\omega^2}. \quad (9)$$

This two-body result serves to disentangle the dissipation due to two-body pair breaking from the genuine many-body bulk viscosity below [10].

In the limit (ii) of high frequency $\omega \gg \varepsilon_F, T$, the contact correlator is evaluated at small times where it factorizes as $\chi(\mathbf{x}, t \rightarrow 0) \simeq m^2 \Gamma(\mathbf{x}, t) \mathcal{C}(0, 0)$; at large frequency, the pair propagator $\Gamma(\mathbf{x}, t)$ approaches the zero-density form [42]. It follows immediately that for $\omega \rightarrow \infty$ the bulk viscosity is proportional to the contact density and decays with a characteristic frequency dependence,

$$\zeta(\omega \rightarrow \infty) = \begin{cases} \frac{C}{4m\omega \ln^2(\omega/\varepsilon_B)} & (2D), \\ \frac{C}{36\pi a^2 (m\omega)^{3/2}} & (3D). \end{cases} \quad (10)$$

This derivation reproduces earlier results [10, 43, 44] in a dramatically simpler calculation. The zero-density results (8) and (9) approach the high-frequency limit with two-body contact density C_0 . However, the exact high-frequency limit is more general and holds at arbitrary density, temperature and interaction in terms of the total contact density $\mathcal{C}(n, T, a)$. This asymptotic behavior is important because it guarantees convergence of the sum rule (7).

Finally, the dynamical bulk viscosity can be computed exactly in the high-temperature limit (iii) by virial expansion [11, 12]. To second order in fugacity $z = e^{\beta\mu}$, the pair distribution $b(\varepsilon) = z^2 e^{-\beta(\varepsilon+2\mu)}$ is combined with

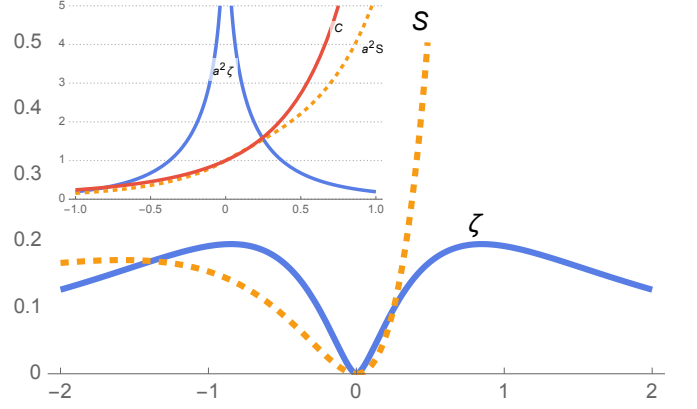


FIG. 2. Bulk viscosity $\zeta(v)$ vs interaction $v = \lambda/a\sqrt{2\pi}$ in the high-temperature limit. Viscosity $\zeta/[2^{3/2}z^2/9\pi\lambda^3]$ (14) (solid blue), sum rule $S/[2^{3/2}z^2T/9\lambda^3]$ (12) (dashed orange). Inset: Contact correlation $a^2\zeta$ (solid blue), contact sum rule a^2S (dashed orange) and contact $C/[16\pi z^2\lambda^{-4}]$ (red).

the zero-density spectral function to yield [42]

$$\zeta_{3D,vir}(\omega > 0) = \frac{2\sqrt{2}}{9} z^2 \lambda^{-3} v^2 \frac{1 - e^{-\beta\omega}}{\beta\omega} \times \left[\Theta(v) 2ve^{v^2} \frac{\sqrt{\beta\omega - v^2} \Theta(\beta\omega - v^2)}{\beta\omega} + \frac{1}{\pi} \int_0^\infty dy \frac{e^{-y} \sqrt{y(y + \beta\omega)}}{(y + v^2)(y + \beta\omega + v^2)} \right]. \quad (11)$$

Here, $v = (\lambda/a)/\sqrt{2\pi}$ denotes the dimensionless interaction parameter as the inverse scattering length in units of the thermal length $\lambda = \sqrt{2\pi/mT}$. The dynamical viscosity has two terms as illustrated in Fig. 1: the first, bound-continuum contribution occurs only on the BEC side $v > 0$ and arises from breaking up bound states at high frequency $|\omega| > \varepsilon_B$, which leads to strong damping as seen before in the two-body limit (9). The second term is the continuum-continuum contribution of dissociated pairs, which extends over all frequencies but has most of its spectral weight at small frequencies $\omega \lesssim \varepsilon_B$. At this order there is no bound-bound contribution because an ideal Bose gas of bound pairs is scale invariant; corrections arise from atom-dimer scattering at order $\mathcal{O}(z^3)$. Both contributions in (11) are necessary to exhaust the sum rule (cf. Fig. 2)

$$S_{3D,vir} = \frac{2\sqrt{2}}{9} z^2 T \lambda^{-3} v^2 \left[(1 + 2v^2) e^{v^2} (1 + \text{erf}(v)) + \frac{2v}{\sqrt{\pi}} - \Theta(v) 4v^2 e^{v^2} \right]. \quad (12)$$

This agrees with the adiabatic derivative (7) of the contact [11, 45] $\mathcal{C}_{3D,vir} = 16\pi z^2 \lambda^{-4} [1 + \sqrt{\pi} v e^{v^2} (1 + \text{erf}(v))]$.

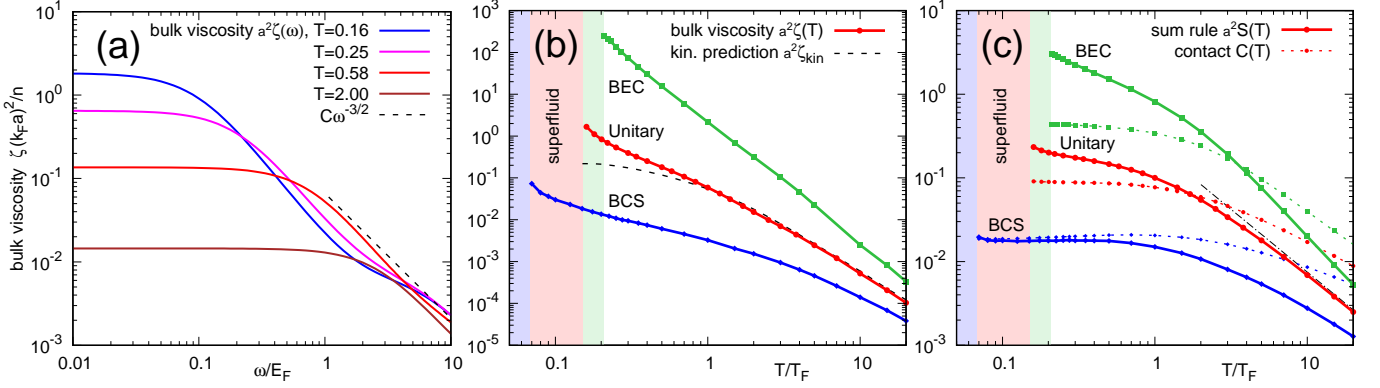


FIG. 3. Bulk viscosity from Luttinger-Ward computation. (a) Dynamical bulk viscosity $\zeta(\omega)(k_F a)^2/\hbar n$ vs frequency ω at unitarity, for increasing temperature from top to bottom (see legend); universal high-frequency tail $\zeta(\omega) \sim C/\omega^{3/2}$ (dashed). (b) dc bulk viscosity $\zeta(T)(k_F a)^2/\hbar n$ vs temperature for different interaction: from top to bottom BEC ($1/k_F a = 1$), Unitary ($1/k_F a = 0$), and BCS ($1/k_F a = -1$). Kinetic prediction $\zeta_{\text{kin}}(T)(k_F a)^2/\hbar n$ (16) from shear viscosity (dashed). (c) Sum rule $S(T)(k_F a)^2/n\varepsilon_F$ (solid) and contact $C(T)/k_F^4$ (dashed) vs temperature for different interaction; virial limit $T^{-3/2}$ (dot-dash).

At unitarity $v \rightarrow 0$, the analytical dynamical viscosity

$$\zeta_{3\text{D},\text{vir}}^{\text{unitary}}(\omega) = \frac{2\sqrt{2}}{9\pi} z^2 \lambda^{-3} v^2 \frac{\sinh(\beta\omega/2)}{\beta\omega/2} K_0(\beta\omega/2). \quad (13)$$

At this order, the unitary contact correlation has a logarithmic singularity $a^2\zeta \sim \ln(T/\omega)z^2$ for small frequencies from the modified Bessel function $K_0(\beta\omega/2)$, as shown in Fig. 1. The logarithmic singularity for small frequencies corresponds via Fourier transform to the logarithmic singularity of the bulk viscosity at long times, $\zeta(t) \sim \ln(t)/(a^2 t)$ [46]. Precisely at unitarity, the bulk viscosity vanishes for all frequencies due to the $v^2 \propto a^{-2}$ factor. Throughout the BEC-BCS crossover, the dc bulk viscosity is then given by (see Fig. 2)

$$\zeta_{3\text{D},\text{vir}}(v) = \frac{2\sqrt{2}}{9\pi} z^2 \lambda^{-3} v^2 [-1 - (1 + v^2)e^{v^2} \text{Ei}(-v^2)]. \quad (14)$$

The exponential integral $\text{Ei}(x)$ yields a logarithmic singularity in scattering length $a^2\zeta \sim \ln(a^2/\lambda^2)z^2$ shown in the inset of Fig. 2. The singular coefficient of the virial expansion is regularized by higher-order terms $\mathcal{O}(z^3)$ from the fermionic self-energy [9, 11]; these are resummed in the Luttinger-Ward computation and yield a finite dc limit in Fig. 3(b) below.

In 2D, there is always a bound state with binding energy $\varepsilon_B > 0$ even for arbitrarily weak attractive interaction. The dynamical bulk viscosity is obtained as [42]

$$\zeta_{2\text{D},\text{vir}}(\omega) = 2\pi z^2 \lambda^{-2} \frac{1 - e^{-\beta\omega}}{\beta\omega} \left[\frac{\beta\varepsilon_B e^{\beta\varepsilon_B} \Theta(\omega - \varepsilon_B)}{\ln^2(\omega/\varepsilon_B - 1) + \pi^2} + \int_0^\infty dy \frac{e^{-y}}{[\ln^2(yT/\varepsilon_B) + \pi^2][\ln^2((yT + \omega)/\varepsilon_B) + \pi^2]} \right].$$

The dc bulk viscosity is then approximately given by

$$\zeta_{2\text{D},\text{vir}}(\varepsilon_B/T) \simeq \frac{2\pi z^2 \lambda^{-2}}{[\ln^2(T/2\varepsilon_B) + \pi^2]^2}. \quad (15)$$

This result for the bulk viscosity based on contact correlations is similar in structure to the fermionic Boltzmann calculation [12] but larger by a factor $4\pi^2$, which is necessary to satisfy the sum rule [42] and the high-frequency asymptotics with the contact density [47, 48] $C_{2\text{D},\text{vir}} = 16\pi^2 z^2 \lambda^{-4} [\beta\varepsilon_B e^{\beta\varepsilon_B} + \int_0^\infty dy \frac{e^{-y}}{\ln^2(yT/\varepsilon_B) + \pi^2}]$.

Luttinger-Ward results.—The Luttinger-Ward (LW) technique is a diagrammatic strong-coupling approach to fermions in the BEC-BCS crossover [49, 50] which treats fermions ψ_σ and the pair field Δ on equal footing. Its predictions for the unitary shear viscosity [9] agree well with recent data [51], and similarly for spin diffusion [52, 53]. In this work, I extend the previous LW approach to compute the bulk viscosity (5) via the contact correlation function (6). It uses the self-consistent pair propagator Γ and includes vertex corrections which represent the scattering between pairs, resummed to arbitrary order [42]. While contact vertex corrections are subleading in the high-temperature limit and could be neglected, they are crucial in the quantum degenerate regime and need to be included for an accurate numerical solution.

The dynamical bulk viscosity $\zeta(\omega)$ determines the dissipation when the scattering length in Eq. (6) is modulated at frequency ω ; the hydrodynamic limit is obtained for $\omega \rightarrow 0$. While $\zeta(\omega)$ vanishes at unitarity as $1/a^2$, the contact correlations $a^2\zeta(\omega)$ are nonzero at unitarity as shown in Fig. 3(a). At low temperature there is a pronounced peak at low frequencies $\omega \lesssim T$ that crosses over into the universal high-frequency tail $\zeta(\omega) \sim C\omega^{-3/2}$ (dashed) for $\omega \gtrsim \varepsilon_F$. At higher $T \gtrsim T_F$ the thermal peak for $\omega \lesssim T$ leads directly into the tail. The peak width $\propto T$ is consistent with quantum critical scaling.

The dc bulk viscosity $a^2\zeta(T)$ shown in Fig. 3(b) is one of the central results: it is largest near the superfluid transition and decreases toward high temperature where pair fluctuations become weaker, as discussed below.

Bulk/shear ratio.—At high temperature kinetic theory predicts the ratio of bulk viscosity ζ to shear viscosity η ,

$$\zeta/\eta \propto (\Pi_{\text{an}}/\Pi_{ii})^2 = [(P - 2\mathcal{E}/3)/P]^2, \quad (16)$$

to be proportional to the squared pressure deviation from scale invariance [11, 54]. Using LW bulk/shear and thermodynamic data [9], this is tested by comparing ζ to the kinetic theory prediction $\zeta_{\text{kin}} \equiv \eta[(P - 2\mathcal{E}/3)/P]^2$, which is shown in Fig. 3(b) as the dashed line. There is very good agreement with unit proportionality factor at high temperature $T \geq T_F$, where a quasiparticle picture is expected to hold. Consequently, the shear viscosity at high temperature is fully determined by scale breaking pair fluctuations as reflected in ζ and in the contact.

In the quantum degenerate regime, the bulk viscosity grows monotonously as the temperature is lowered toward the superfluid phase transition and can reach large values $\zeta \gtrsim \hbar n$ near T_c . At low temperature, $\zeta > \zeta_{\text{kin}}$ and also $\zeta/\eta > 1$ can exceed unity since pair fluctuations near the superfluid phase transition affect the bulk viscosity more strongly than the shear viscosity.

Critical pair fluctuations.—The fact that the bulk viscosity is the dynamical correlator of order-parameter fluctuations $\Delta(\mathbf{x}, t)$ suggests that ζ might diverge at T_c [29]; instead, vertex corrections in the LW calculation substantially reduce the contact vertex at low momenta and render the bulk viscosity large but finite [42]. The absence of divergent critical scaling might depend on how the critical point is approached, as found in QCD [55].

Finally, Fig. 3(c) shows the viscosity sum rule S . It is large in the quantum degenerate regime and decreases toward high temperature as $T^{-3/2}$ (12) (dot-dashed), i.e., faster than the contact $\mathcal{C} \sim T^{-1}$ itself (dashed) [9, 45, 56].

To conclude, the bulk viscosity identifies the breaking of scale invariance with the strength of pair fluctuations, which become very large near T_c and on the BEC side. This provides a strong signature in cold atom experiments, either directly in the response of the contact [14, 38, 39] to a change in scattering length, or by modulating the scattering length periodically and measuring the dissipative heating rate $\dot{\mathcal{E}} = d^2 a^2 \zeta \cdot (\partial_t a^{-1})^2$ [14] proportional to $a^2 \zeta(\omega, T)$ shown in Fig. 3(a,b), which is nonzero also at unitarity. Further signatures of enhanced dissipation ζ can be found in the hydrodynamic description of scaling or breathing dynamics [10, 13, 18, 21] and sound attenuation $D_s = [\frac{4}{3}\eta + \zeta + \kappa(c_v^{-1} - c_p^{-1})]/mn$ [2, 57].

Note added. After submission, two other calculations [58, 59] of the bulk viscosity in the high-temperature limit appeared, which agree with our results where applicable.

Acknowledgments. I acknowledge fruitful discussions with M. Bluhm, G. Bruun, J. Hofmann, M. Horikoshi,

S. Jochim, Y. Nishida, J. Pawłowski, T. Schäfer, J. Thywissen, W. Zwerger, and M. W. Zwierlein. This work is supported by Deutsche Forschungsgemeinschaft (DFG) via Collaborative Research Centre “SFB1225” (ISO-QUANT) and under Germanys Excellence Strategy “EXC-2181/1-390900948” (Heidelberg STRUCTURES Excellence Cluster).

-
- [1] L. D. Landau and E. M. Lifshitz, *Fluid Mechanics* (Butterworth-Heinemann, Oxford, 1987).
 - [2] D. Forster, *Hydrodynamic fluctuations, broken symmetry, and correlation functions* (WA Benjamin, Reading, 1975).
 - [3] D. T. Son, Vanishing bulk viscosities and conformal invariance of the unitary Fermi gas, *Phys. Rev. Lett.* **98**, 020604 (2007).
 - [4] F. Karsch, D. Kharzeev, and K. Tuchin, Universal properties of bulk viscosity near the QCD phase transition, *Phys. Lett. B* **663**, 217 (2008).
 - [5] G. D. Moore and O. Saremi, Bulk viscosity and spectral functions in QCD, *J. High Energy Phys.* **2008** (09), 015.
 - [6] P. Romatschke and D. T. Son, Spectral sum rules for the quark-gluon plasma, *Phys. Rev. D* **80**, 065021 (2009).
 - [7] Y. Akamatsu, A. Mazeliauskas, and D. Teaney, Bulk viscosity from hydrodynamic fluctuations with relativistic hydrokinetic theory, *Phys. Rev. C* **97**, 024902 (2018).
 - [8] E. Taylor and M. Randeria, Viscosity of strongly interacting quantum fluids: spectral functions and sum rules, *Phys. Rev. A* **81**, 053610 (2010).
 - [9] T. Enss, R. Haussmann, and W. Zwerger, Viscosity and scale invariance in the unitary Fermi gas, *Ann. Phys. (N.Y.)* **326**, 770 (2011).
 - [10] E. Taylor and M. Randeria, Apparent low-energy scale invariance in two-dimensional Fermi gases, *Phys. Rev. Lett.* **109**, 135301 (2012).
 - [11] K. Dusling and T. Schäfer, Bulk viscosity and conformal symmetry breaking in the dilute Fermi gas near unitarity, *Phys. Rev. Lett.* **111**, 120603 (2013).
 - [12] C. Chafin and T. Schäfer, Scale breaking and fluid dynamics in a dilute two-dimensional Fermi gas, *Phys. Rev. A* **88**, 043636 (2013).
 - [13] E. Elliott, J. A. Joseph, and J. E. Thomas, Observation of conformal symmetry breaking and scale invariance in expanding Fermi gases, *Phys. Rev. Lett.* **112**, 040405 (2014).
 - [14] K. Fujii and Y. Nishida, Hydrodynamics with spacetime-dependent scattering length, *Phys. Rev. A* **98**, 063634 (2018).
 - [15] L. P. Pitaevskii and A. Rosch, Breathing modes and hidden symmetry of trapped atoms in two dimensions, *Phys. Rev. A* **55**, R853 (1997).
 - [16] M. Olshanii, H. Perrin, and V. Lorent, Example of a quantum anomaly in the physics of ultracold gases, *Phys. Rev. Lett.* **105**, 095302 (2010).
 - [17] J. Hofmann, Quantum Anomaly, Universal Relations, and Breathing Mode of a Two-Dimensional Fermi Gas, *Phys. Rev. Lett.* **108**, 185303 (2012).
 - [18] E. Vogt, M. Feld, B. Fröhlich, D. Pertot, M. Koschorreck, and M. Köhl, Scale invariance and viscosity of a

- two-dimensional Fermi gas, *Phys. Rev. Lett.* **108**, 070404 (2012).
- [19] M. Holten, L. Bayha, A. C. Klein, P. A. Murthy, P. M. Preiss, and S. Jochim, Anomalous breaking of scale invariance in a two-dimensional Fermi gas, *Phys. Rev. Lett.* **121**, 120401 (2018).
- [20] T. Peppler, P. Dyke, M. Zamorano, I. Herrera, S. Hoinka, and C. J. Vale, Quantum anomaly and 2D-3D crossover in strongly interacting Fermi gases, *Phys. Rev. Lett.* **121**, 120402 (2018).
- [21] P. A. Murthy, N. Defenu, L. Bayha, M. Holten, P. M. Preiss, T. Enss, and S. Jochim, Quantum scale anomaly and spatial coherence in a 2D Fermi superfluid, *Science* **365**, 268 (2019).
- [22] A. S. Dukhin and P. J. Goetz, Bulk viscosity and compressibility measurement using acoustic spectroscopy, *J. Chem. Phys.* **130**, 124519 (2009).
- [23] M. Martinez and T. Schäfer, Hydrodynamic tails and a fluctuation bound on the bulk viscosity, *Phys. Rev. A* **96**, 063607 (2017).
- [24] A. Czajka and S. Jeon, Kubo formulas for the shear and bulk viscosity relaxation times and the scalar field theory shear τ_π calculation, *Phys. Rev. C* **95**, 064906 (2017).
- [25] M. A. Escobedo, M. Mannarelli, and C. Manuel, Bulk viscosities for cold Fermi superfluids close to the unitary limit, *Phys. Rev. A* **79**, 063623 (2009).
- [26] Y.-H. Hou, L. P. Pitaevskii, and S. Stringari, Scaling solutions of the two-fluid hydrodynamic equations in a harmonically trapped gas at unitarity, *Phys. Rev. A* **87**, 033620 (2013).
- [27] W. Zwerger, ed., *The BCS-BEC Crossover and the Unitary Fermi Gas*, Lecture Notes in Physics Vol. 836 (Springer, Berlin, 2012).
- [28] F. Werner and Y. Castin, Unitary gas in an isotropic harmonic trap: Symmetry properties and applications, *Phys. Rev. A* **74**, 053604 (2006).
- [29] A. Onuki, *Phase Transition Dynamics* (Cambridge University Press, Cambridge, 2002).
- [30] P. Nikolić and S. Sachdev, Renormalization-group fixed points, universal phase diagram, and $1/N$ expansion for quantum liquids with interactions near the unitarity limit, *Phys. Rev. A* **75**, 033608 (2007).
- [31] S. Sachdev, *Quantum Phase Transitions* (Cambridge University Press, Cambridge, 2011).
- [32] T. Enss, Quantum critical transport in the unitary Fermi gas, *Phys. Rev. A* **86**, 013616 (2012).
- [33] L. P. Kadanoff and J. Swift, Transport coefficients near the liquid-gas critical point, *Phys. Rev.* **166**, 89 (1968).
- [34] L. P. Kadanoff and P. C. Martin, Hydrodynamic equations and correlation functions, *Ann. Phys. (N.Y.)* **24**, 419 (1963).
- [35] L. D. Landau and E. M. Lifshitz, *Statistical Mechanics, Part II* (Pergamon Press, New York, 1981).
- [36] W. Zwerger, Strongly Interacting Fermi Gases, in *Quantum Matter at Ultralow Temperatures*, Vol. 191, edited by M. Inguscio, W. Ketterle, S. Stringari, and G. Roati (IOS Press, Amsterdam, 2016) 1608.00457.
- [37] S. Tan, Energetics of a strongly correlated Fermi gas, *Ann. Phys. (N.Y.)* **323**, 2952 (2008).
- [38] A. B. Bardon, S. Beattie, C. Luciuk, W. Cairncross, D. Fine, N. S. Cheng, G. J. A. Edge, E. Taylor, S. Zhang, S. Trotzky, and J. H. Thywissen, Transverse Demagnetization Dynamics of a Unitary Fermi Gas, *Science* **344**, 722 (2014).
- [39] C. Luciuk, S. Smale, F. Böttcher, H. Sharum, B. A. Olsen, S. Trotzky, T. Enss, and J. H. Thywissen, Observation of quantum-limited spin transport in strongly interacting two-dimensional Fermi gases, *Phys. Rev. Lett.* **118**, 130405 (2017).
- [40] F. Werner and Y. Castin, General relations for quantum gases in two and three dimensions. Two-component fermions, *Phys. Rev. A* **86**, 013626 (2012).
- [41] P. A. Murthy, M. Neidig, R. Klemt, L. Bayha, I. Boettcher, T. Enss, M. Holten, G. Zürn, P. M. Preiss, and S. Jochim, High-temperature pairing in a strongly interacting two-dimensional Fermi gas, *Science* **359**, 452 (2018).
- [42] Supplemental Material.
- [43] J. Hofmann, Current response, structure factor and hydrodynamic quantities of a two- and three-dimensional Fermi gas from the operator-product expansion, *Phys. Rev. A* **84**, 043603 (2011).
- [44] W. D. Goldberger and Z. U. Khandker, Viscosity sum rules at large scattering lengths, *Phys. Rev. A* **85**, 013624 (2012).
- [45] Z. Yu, G. M. Bruun, and G. Baym, Short-range correlations and entropy in ultracold-atom Fermi gases, *Phys. Rev. A* **80**, 023615 (2009).
- [46] J. Maki and F. Zhou, Quantum Many-Body Conformal Dynamics: Symmetries, Geometry, Conformal Tower States, and Entropy Production, *Phys. Rev. A* **100**, 023601 (2019).
- [47] V. Ngampruetikorn, J. Levinsen, and M. M. Parish, Pair Correlations in the Two-Dimensional Fermi Gas, *Phys. Rev. Lett.* **111**, 265301 (2013).
- [48] M. Barth and J. Hofmann, Pairing effects in the nondegenerate limit of the two-dimensional Fermi gas, *Phys. Rev. A* **89**, 013614 (2014).
- [49] R. Haussmann, W. Rantner, S. Cerrito, and W. Zwerger, Thermodynamics of the BCS-BEC crossover, *Phys. Rev. A* **75**, 023610 (2007).
- [50] M. Bauer, M. M. Parish, and T. Enss, Universal Equation of State and Pseudogap in the Two-Dimensional Fermi Gas, *Phys. Rev. Lett.* **112**, 135302 (2014).
- [51] M. Bluhm, J. Hou, and T. Schäfer, Determination of the density and temperature dependence of the shear viscosity of a unitary Fermi gas based on hydrodynamic flow, *Phys. Rev. Lett.* **119**, 065302 (2017).
- [52] T. Enss and R. Haussmann, Quantum Mechanical Limitations to Spin Transport in the Unitary Fermi Gas, *Phys. Rev. Lett.* **109**, 195303 (2012).
- [53] T. Enss and J. H. Thywissen, Universal Spin Transport and Quantum Bounds for Unitary Fermions, *Annu. Rev. Condens. Matter Phys.* **10**, 85106 (2019).
- [54] M. Bluhm, B. Kämpfer, and K. Redlich, Ratio of bulk to shear viscosity in a quagluon plasma: from weak to strong coupling, *Phys. Lett. B* **709**, 77 (2012).
- [55] M. Martinez, T. Schäfer, and V. Skokov, Critical behavior of the bulk viscosity in QCD, *Phys. Rev. D* **100**, 074017 (2019).
- [56] B. Mukherjee, P. B. Patel, Z. Yan, R. J. Fletcher, J. Struck, and M. W. Zwierlein, Spectral response and contact of the unitary Fermi gas, *Phys. Rev. Lett.* **122**, 203402 (2019).
- [57] P. B. Patel, Z. Yan, B. Mukherjee, R. J. Fletcher, J. Struck, and M. W. Zwierlein, Universal Sound Diffusion in a Strongly Interacting Fermi Gas, *arXiv:1909.02555* (2019).

- [58] Y. Nishida, Viscosity spectral functions of resonating fermions in the quantum virial expansion, *Ann. Phys. (N.Y.)* **410**, 167949 (2019).
 [59] J. Hofmann, High-temperature expansion of the viscosity in interacting quantum gases, arXiv:1905.05133 (2019).

Supplemental material

Contact correlations

The contact correlation can be written in terms of the pair field $\Delta(\mathbf{x}, \tau)$ in imaginary time τ as

$$\chi(\mathbf{x}, \tau) = \langle \Delta^\dagger \Delta(\mathbf{x}, \tau) \Delta^\dagger \Delta(0, 0) \rangle \quad (17)$$

with imaginary time ordering understood. The pair propagator $\langle \Delta(\mathbf{x}, \tau) \Delta^\dagger(0, 0) \rangle = m^2 \Gamma(\mathbf{x}, \tau)$ can be expressed in terms of the T matrix $\Gamma(\mathbf{x}, \tau)$, and one can write the contact correlation as the scale variation of the T matrix,

$$\begin{aligned} \chi(\mathbf{x}, \tau) &= \frac{m^2}{c_d} \frac{\delta \Gamma(\mathbf{x}, \tau)}{\delta \ln |a(0, 0)|} \\ &= m^4 \Gamma(\mathbf{x}, \tau) \Gamma(-\mathbf{x}, -\tau) + \text{vertex corrections.} \end{aligned} \quad (18)$$

In imaginary Matsubara frequency $i\omega_m$, the spatially integrated contact correlator is given by

$$\begin{aligned} X(i\omega_m) &= \int d^d x \chi(\mathbf{x}, i\omega_m) \\ &= \frac{m^4}{\beta V} \sum_{\mathbf{q} \varepsilon_n} \Gamma(\mathbf{q}, i\varepsilon_n) \Gamma(\mathbf{q}, i\varepsilon_n + i\omega_m) + \text{vtx. corr.}, \end{aligned} \quad (19)$$

while the contact density itself is given by $\mathcal{C} = (m^2/\beta V) \sum_{\mathbf{q} \varepsilon_n} \Gamma(\mathbf{q}, i\varepsilon_n)$. The vertex corrections are important in the quantum degenerate case and are computed below using the Luttinger-Ward approach. At high temperature or low density, the vertex corrections are subleading and the first term can be computed analytically. After analytical continuation to real frequency, the retarded correlator reads

$$\begin{aligned} X^R(\omega) &= \frac{m^4}{V} \sum_{\mathbf{q}} \int d\varepsilon A(\mathbf{q}, \varepsilon) b(\varepsilon) \\ &\times [\Gamma^R(\mathbf{q}, \varepsilon + \omega) + \Gamma^A(\mathbf{q}, \varepsilon - \omega)] + \text{vtx. corr.} \end{aligned} \quad (20)$$

in terms of the retarded/advanced pair propagators and the pair spectral function $A(\mathbf{q}, \varepsilon) = -(1/\pi) \text{Im} \Gamma^R(\mathbf{q}, \varepsilon)$. This determines the dynamical bulk viscosity as the contact correlator spectral function

$$\begin{aligned} \frac{d^2}{c_d^2} \zeta(\omega) &= -\frac{\text{Im} X^R(\omega)}{\omega} \\ &= \frac{\pi m^4}{\omega V} \sum_{\mathbf{q}} \int_{-\infty}^{\infty} d\varepsilon A(\mathbf{q}, \varepsilon) A(\mathbf{q}, \varepsilon + \omega) [b(\varepsilon) - b(\varepsilon + \omega)] \\ &\quad + \text{vtx. corr.} \end{aligned} \quad (21)$$

Zero-density limit

At zero density, the vertex corrections in (19) vanish and the contact correlator is completely determined by the particle-hole excitations of pairs (21). The pair propagator (T matrix), in turn, is given diagrammatically by repeated particle-particle scattering,

$$\Gamma^R(\mathbf{q}, \varepsilon)^{-1} = g_0^{-1} - \int \frac{d^d p}{(2\pi)^d} \frac{1 - f(\xi_{\mathbf{p}}) - f(\xi_{\mathbf{q}-\mathbf{p}})}{\varepsilon + i0 - \xi_{\mathbf{p}} - \xi_{\mathbf{q}-\mathbf{p}}}. \quad (22)$$

Here, $f(\varepsilon)$ denotes the Fermi distribution and $\xi_{\mathbf{p}} = \varepsilon_{\mathbf{p}} - \mu$ measures the dispersion $\varepsilon_{\mathbf{p}} = p^2/2m$ from the chemical potential μ . At zero density there is only a single up and a single down fermion, such that the Fermi functions $f(\xi_{\mathbf{p}})$ vanish: the momentum integral is then performed analytically and yields the pair spectral functions $A(\mathbf{q}, \varepsilon) = -(1/\pi) \text{Im} \Gamma^R(\mathbf{q}, \varepsilon)$ given as

$$\begin{aligned} A_{2D}(\mathbf{q}, \varepsilon) &= \frac{4\pi}{m} \left[\varepsilon_B \delta(\varepsilon + 2\mu + \varepsilon_B - \omega_q) \right. \\ &\quad \left. + \frac{\Theta(\varepsilon + 2\mu - \omega_q)}{\ln^2[(\varepsilon + 2\mu - \omega_q)/\varepsilon_B] + \pi^2} \right], \end{aligned} \quad (23)$$

$$\begin{aligned} A_{3D}(\mathbf{q}, \varepsilon) &= \frac{4\pi}{m^{3/2}} \left[2\sqrt{\varepsilon_B} \delta(\varepsilon + 2\mu + \varepsilon_B - \omega_q) \Theta(a) \right. \\ &\quad \left. + \frac{1}{\pi} \frac{\sqrt{\varepsilon + 2\mu - \omega_q} \Theta(\varepsilon + 2\mu - \omega_q)}{\varepsilon + 2\mu + (ma^2)^{-1} - \omega_q} \right]. \end{aligned} \quad (24)$$

The first term is the bound-state peak, which appears always for attractive interaction in 2D and for $a > 0$ (BEC side) in 3D, followed by the scattering continuum; $\omega_q = q^2/2M$ denotes the dispersion of fermion pairs (molecular bound states) of mass $M = 2m$.

In order to compute the bulk viscosity in the zero-density limit, one has to set $T = 0$ and chemical potential $\mu = -\varepsilon_B/2$ at the threshold of the two-body binding energy $\varepsilon_B = \hbar^2/ma^2$ ($\mu = 0$ when there is no two-body bound state on the BCS side in 3D). At zero density, dissociating a bound state at $\varepsilon = \omega_q = 0$ in 2D yields Eq. (8) in the main text. This satisfies the sum rule (7), $S_{2D, \text{vac}} = \mathcal{C}_0/4\pi m = \varepsilon_B/V = -(1/4)(\partial^2 \mathcal{E}_0/\partial(\ln |a|)^2)_s$ where $\mathcal{E}_0 = -\mathcal{C}_0/4\pi m$. In 3D, a vacuum bound state exists only for $a > 0$, and one finds Eq. (9), which again satisfies the sum rule (7) with $S_{3D, \text{vac}} = \mathcal{C}_0/36\pi ma = -(1/9)(\partial^2 \mathcal{E}_0/\partial(\ln |a|)^2)_s$ and $\mathcal{E}_0 = -\mathcal{C}_0/8\pi ma$.

High-frequency limit

The response at high frequencies is only sensitive to the behavior of the contact correlation at short times, which factorizes in the limit $\tau \rightarrow 0$ as

$$\begin{aligned} \chi(\mathbf{x}, \tau) &= \langle \Delta^\dagger \Delta(\mathbf{x}, \tau) \Delta^\dagger \Delta(0, 0) \rangle \\ &\simeq \langle \Delta(\mathbf{x}, \tau) \Delta^\dagger(0, 0) \rangle \langle \Delta^\dagger \Delta(0, 0) \rangle \\ &= m^2 \Gamma(\mathbf{x}, \tau) \mathcal{C}(0, 0). \end{aligned}$$

In this limit, the T matrix $\Gamma(\mathbf{x}, \tau)$ is unaffected by finite density and approaches the zero-density form (23), (24). Therefore, the high-frequency limit $\omega \rightarrow \infty$ of the bulk viscosity is proportional to the contact density and decays with the asymptotic frequency dependence (10) quoted in the main text for $\omega \gg \varepsilon_B$.

Virial expansion

The virial expansion to second order $\mathcal{O}(z^2)$ in the fermionic fugacity $z = e^{\beta\mu}$ correctly describes the properties of the interacting Fermi gas as long as the pair fugacity $z_{\text{pair}} = z^2 e^{\beta\varepsilon_B} \ll 1$ remains small. Because vertex corrections in Eq. (21) appear only at higher order in z , the second-order virial result is fully determined by the first term in that equation. Since the occupation factor $b(\varepsilon)$ is already order z^2 , it suffices to use the zero-density form of the pair spectral function (24) and the Boltzmann distribution to obtain

$$\frac{d^2}{c_d^2} \zeta(\omega) = \frac{\pi m^4}{\omega} \int \frac{d^3 q}{(2\pi)^3} \int d\varepsilon A_{3D}(\mathbf{q}, \varepsilon) A_{3D}(\mathbf{q}, \varepsilon + \omega) \times z^2 e^{-\beta(\varepsilon+2\mu)} [1 - e^{-\beta\omega}].$$

With the explicit form of A_{3D} (24) and in the new frequency variable $y = \beta(\varepsilon + 2\mu - \omega_q)$ one finds

$$\frac{d^2}{c_d^2} \zeta(\omega) = 16\pi^3 m z^2 \frac{1 - e^{-\beta\omega}}{\omega} \int \frac{d^3 q}{(2\pi)^3} e^{-\beta\omega_q} \int dy e^{-y} \times \left[2\sqrt{\beta\varepsilon_B} \delta(y + \beta\varepsilon_B) \Theta(v) + \frac{1}{\pi} \frac{\sqrt{y} \Theta(y)}{y + v^2} \right] [y \mapsto y + \beta\omega],$$

where $v = (\lambda/a\sqrt{2\pi})$ denotes the dimensionless 3D interaction parameter. Since $\zeta(\omega)$ is even in frequency it suffices to consider $\omega > 0$; then there is the bound-continuum contribution from the bound state $y = -\beta\varepsilon_B$ in the first bracket and the continuum $y + \beta\omega > 0$ in the second. On the other hand, for $y > 0$ one obtains the continuum-continuum contribution, and both terms are combined to yield

$$\frac{d^2}{c_d^2} \zeta(\omega) = 32\sqrt{2}\pi^2 m z^2 \lambda^{-3} \frac{1 - e^{-\beta\omega}}{\omega} \times \left[2ve^{v^2} \Theta(v) \frac{\sqrt{\beta(\omega - \varepsilon_B)} \Theta(\omega - \varepsilon_B)}{\beta\omega} + \frac{1}{\pi} \int_0^\infty dy \frac{e^{-y} \sqrt{y(y + \beta\omega)}}{(y + v^2)(y + \beta\omega + v^2)} \right].$$

Note that there appears no bound-bound contribution $\delta(\omega)$ because an ideal Bose gas of pairs is scale invariant. Multiplication with the coefficient $(c_d/d)^2 = T^2 \lambda^2 v^2 / (288\pi^3)$ in 3D yields the dynamical bulk viscosity (11).

Frequency integration determines the spectral weight of the terms in brackets as $S_{bc} = [2(1 + 2v^2)e^{v^2} \text{erf}(v) - 4v^2 e^{v^2} + 4v/\sqrt{\pi}] \Theta(v)$ for the bound-continuum contribution, which becomes large in the BEC limit. Furthermore, the continuum-continuum contribution has weight $S_{cc} = [(1 + 2v^2)e^{v^2}(1 - \text{erf}(|v|)) - 2|v|/\sqrt{\pi}]$, and by combining both one exhausts the sum rule (12).

The contact density is given to the same order in the virial expansion by the occupied spectral function of pairs,

$$\mathcal{C}_{3D, \text{vir}} = m^2 \int \frac{d^3 q}{(2\pi)^3} \int_{-\infty}^\infty d\varepsilon A(\mathbf{q}, \varepsilon) b(\varepsilon) = 16\pi z^2 \lambda^{-4} \left[1 + \sqrt{\pi} v e^{v^2} (1 + \text{erf}(v)) \right].$$

This is equivalent to the derivative of the second virial coefficient, $\mathcal{C} = 8\pi\sqrt{2}\pi z^2 \lambda^{-4} \partial b_2(v)/\partial v$ with $b_2(v) = -1/4\sqrt{2} + (1/\sqrt{2})(1 + \text{erf } v)e^{v^2}$, $b'_2 = \sqrt{2/\pi} + 2vb_2$, and $b''_2 = 2(b_2 + vb'_2)$. The contact grows monotonously with the interaction parameter v , as shown in Fig. 2; this generalizes earlier results [11, 45].

In order to compute the adiabatic derivative of the contact, one has to keep the entropy per particle $s = \beta(h - \mu)$ fixed. This is given in terms of the enthalpy per particle $h = (p + \mathcal{E})/n$ and the chemical potential μ , and at second order virial expansion one finds

$$s = \frac{5}{2} \frac{1 + z(b_2 - vb'_2/5)}{1 + 2zb_2} - \ln(z)$$

in extension of the Sackur-Tetrode entropy formula $s = 5/2 - \ln(z)$. The adiabatic derivative with respect to v is related to the grand canonical derivative keeping μ and T fixed, plus an additional term adjusting z'/z to compensate for the change in entropy: $(\partial z^2 b'_2 / \partial v)_s = (2 \frac{z'}{z} b'_2 + b''_2) z^2$. In the BEC limit, $z'/z = -v$ and we find the adiabatic derivative $(\partial z^2 b'_2 / \partial v)_s = 2z^2 b_2$. The corresponding two-body contact is $\mathcal{C}_0 = 4\pi n/a = 16\pi z^2 \lambda^{-4} \sqrt{\pi} 2ve^{v^2}$, and the adiabatic derivative $(\partial \mathcal{C}_0 / \partial v)_s = \mathcal{C}_0/v = 16\pi z^2 \lambda^{-4} \sqrt{\pi} 2e^{v^2}$ yields the bound-continuum contribution to the sum rule (12) *without a bound-bound contribution*. Similarly, the adiabatic derivative of the continuum part of the contact at fixed fermionic entropy $s = 5/2 - \ln(z)$ yields the continuum-continuum contribution to the sum rule (12), thus confirming Eq. (7) by explicit computation in the high-temperature limit.

The dynamical bulk viscosity in *two dimensions* is computed in a completely analogous fashion to obtain the bulk viscosity quoted in the main text. Its total spectral weight is given by the sum rule (7) with

$$S_{2D, \text{vir}} = 2z^2 T \lambda^{-2} \left[\beta\varepsilon_B e^{\beta\varepsilon_B} + 2 \int_0^\infty dy \frac{e^{-y} \ln(y/\beta\varepsilon_B)}{[\ln^2(y/\beta\varepsilon_B) + \pi^2]^2} \right].$$

The sum rule agrees with the adiabatic derivative of the contact density [47, 48]

$$\mathcal{C}_{2D, \text{vir}} = 16\pi^2 z^2 \lambda^{-4} \left[\beta \varepsilon_B e^{\beta \varepsilon_B} + \int_0^\infty dy \frac{e^{-y}}{\ln^2(y/\beta \varepsilon_B) + \pi^2} \right].$$

Luttinger-Ward approach

The Luttinger-Ward approach [49] to the attractive Fermi gas is based on two-component fermions $\psi_\sigma(\mathbf{x}, \tau)$ which interact by forming (virtual) pairs $\Delta(\mathbf{x}, \tau)$. It is constructed to be a conserving approximation which exactly conserves not only particle number and momentum current but also the dilatation current (scale invariance) [9] and the Tan relations [32]. The pair propagator is given by the T matrix (cf. Eq. (22))

$$\Gamma^{-1}(\mathbf{q}, i\epsilon_n) = g_0^{-1} + M(\mathbf{q}, i\epsilon_n) \quad (25)$$

with bare coupling g_0 , and the pair self-energy is given by the fermion particle-particle bubble $M(\mathbf{q}, i\epsilon_n)$. This is a convolution of two *dressed* fermion propagators $G(\mathbf{q}, i\epsilon_n)$ in momentum \mathbf{q} and Matsubara frequency $i\epsilon_n$. However, numerically it is more conveniently computed by a Fourier transform to real space \mathbf{r} and imaginary time τ , where the particle-particle bubble is a local product

$$M(\mathbf{r}, \tau) = [G(\mathbf{r}, \tau)]^2; \quad (26)$$

the resulting $M(\mathbf{r}, \tau)$ is then Fourier transformed back to momentum and frequency $M(\mathbf{q}, i\epsilon_n)$ to be inserted in the pair Dyson equation (25). In turn, the fermion propagator for each spin component of the balanced gas is given by the Dyson equation

$$G^{-1}(\mathbf{q}, i\epsilon_n) = -i\epsilon_n + \varepsilon_q - \mu + \Sigma(\mathbf{q}, i\epsilon_n) \quad (27)$$

with the fermionic self-energy $\Sigma(\mathbf{q}, i\epsilon_n)$ determined by scattering fermions off virtual pairs. The particle-hole bubble of a pair (particle) and a fermion (hole) is again concisely written as a local multiplication in Fourier space,

$$\Sigma(\mathbf{r}, \tau) = \Gamma(\mathbf{r}, \tau)G(-\mathbf{r}, -\tau). \quad (28)$$

These four equations (25)–(28) form a closed set of equations, which is solved self-consistently by iteration until convergence is reached. The propagators $\Gamma(\mathbf{q}, i\epsilon_n)$ and $G(\mathbf{q}, i\epsilon_n)$ are first initialized with the bare propagators, then Fourier transformed to real space. The self-energies (26) and (28) are computed in real space, then Fourier transformed back to momentum space. These are then inserted into the Dyson equations (25) and (27), which provide the starting point for the next iteration.

The Luttinger-Ward approach has previously been used for fermionic shear and spin transport [9, 52]; by considering the response to variations of an external field (shear strain or spin gradient), a new set of self-consistent transport equations is obtained for the renormalized current vertices which include vertex corrections to satisfy the Ward identities exactly. For the bosonic contact correlations, instead, one has to consider the response to a time-dependent scale variation. Specifically, the scale breaking variation $\delta = -\partial/\partial(4\pi m a)^{-1}$ at external drive frequency $i\omega_m$ of each of the above equations (25)–(28) yields a new set of self-consistent transport equations for the renormalized trace anomaly response vertices:

$$\delta\Gamma^{-1}(\mathbf{q}, i\epsilon_n; i\omega_m) = \delta g_0^{-1} + \delta M(\mathbf{q}, i\epsilon_n; i\omega_m), \quad (29)$$

$$\delta M(\mathbf{r}, \tau; i\omega_m) = 2G(\mathbf{r}, \tau; i\omega_m) \delta G(\mathbf{r}, \tau; i\omega_m), \quad (30)$$

$$\begin{aligned} \delta G^{-1}(\mathbf{q}, i\epsilon_n; i\omega_m) &= \delta G_0^{-1}(\mathbf{q}, i\epsilon_n; i\omega_m) \\ &\quad + \delta \Sigma_{\text{MT}}(\mathbf{q}, i\epsilon_n; i\omega_m) \\ &\quad + \delta \Sigma_{\text{AL}}(\mathbf{q}, i\epsilon_n; i\omega_m), \end{aligned} \quad (31)$$

$$\delta \Sigma_{\text{MT}}(\mathbf{r}, \tau; i\omega_m) = \Gamma(\mathbf{r}, \tau; i\omega_m) \delta G(-\mathbf{r}, -\tau; i\omega_m), \quad (32)$$

$$\delta \Sigma_{\text{AL}}(\mathbf{r}, \tau; i\omega_m) = \delta \Gamma(\mathbf{r}, \tau; i\omega_m) G(-\mathbf{r}, -\tau; i\omega_m). \quad (33)$$

In the first line (29), $\delta\Gamma^{-1}$ denotes the interaction scale variation of the bosonic pair propagator: it consists of the bare contact vertex $\delta g_0^{-1} = -m^2$, which is obtained from the scale variation c_d of the bare coupling, and the contact vertex correction δM , which arises from the scale variation of the particle-particle bubble (30). While the bare fermionic propagator has no scale dependence, $\delta G_0^{-1} = 0$, the dressed fermion propagator (27) acquires a scale dependence from the self-energy term (28). This gives rise to a *fermionic* trace anomaly vertex δG^{-1} in (31) with two distinct types of vertex corrections. The first, so-called Maki-Thompson vertex correction $\delta \Sigma_{\text{MT}}$ in (32) is built from a fermionic anomaly vertex δG , while the second, Aslamazov-Larkin vertex corrections $\delta \Sigma_{\text{AL}}$ in (33) arises from the renormalized bosonic contact vertex $\delta \Gamma$. The scale variation of the propagators is computed from the inverse propagators as

$$\begin{aligned} \delta G(\mathbf{q}, i\epsilon_n; i\omega_m) &= -G(\mathbf{q}, i\epsilon_n) \delta G^{-1}(\mathbf{q}, i\epsilon_n; i\omega_m) \\ &\quad \times G(\mathbf{q}, i\epsilon_n + i\omega_m), \end{aligned}$$

$$\begin{aligned} \delta \Gamma(\mathbf{q}, i\epsilon_n; i\omega_m) &= -\Gamma(\mathbf{q}, i\epsilon_n) \delta \Gamma^{-1}(\mathbf{q}, i\epsilon_n; i\omega_m) \\ &\quad \times \Gamma(\mathbf{q}, i\epsilon_n + i\omega_m). \end{aligned}$$

The self-consistent transport equations are solved separately for each value of the external frequency $i\omega_m$; as before, a Fourier transform converts the anomaly vertices between Fourier space $(\mathbf{q}, i\epsilon_n)$ and real space (\mathbf{r}, τ) at fixed parameter $i\omega_m$.

In the first iteration of the transport equations, only the bare pair propagator depends on scale and

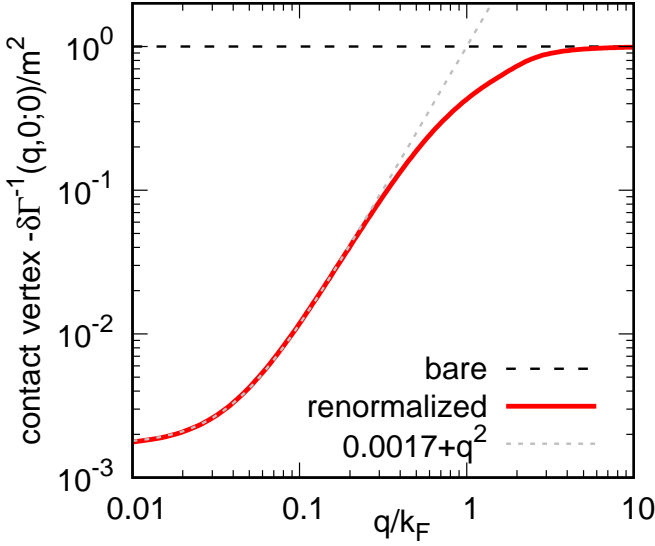


FIG. 4. Renormalized contact vertex. The static contact vertex near T_c is strongly suppressed by contact vertex corrections as $\sim q^2$ at low momenta q . Luttinger-Ward data are shown for reduced temperature $(T - T_c)/T_c = 0.003$.

yields the bare contact vertex $\delta g_0^{-1} = -m^2$, while the bare fermions are independent of the interaction scale, $\delta G_0^{-1}(\mathbf{q}, i\epsilon_n; i\omega_m) = 0$. In subsequent iterations, the fermionic anomaly vertex δG^{-1} picks up an interaction scale dependence from the MT and AL vertex corrections (32) and (33). The scale dependence of the fermionic vertex, in turn, generates vertex corrections δM which renormalize the contact vertex $\delta \Gamma^{-1}$. Once convergence is reached, the Maki-Thompson and Aslamazov-Larkin vertex corrections include contributions of arbitrarily high perturbative order in the bare coupling.

The spatially integrated contact correlation function (19) is computed by the Kubo formula

$$\begin{aligned} \chi(\mathbf{k} = 0, i\omega_m) &= X(i\omega_m) \\ &= \frac{1}{\beta V} \sum_{\mathbf{q}\epsilon_n} \delta g_0^{-1} \Gamma(\mathbf{q}, i\epsilon_n) \delta \Gamma^{-1}(\mathbf{q}, i\epsilon_n; i\omega_m) \Gamma(\mathbf{q}, i\epsilon_n + i\omega_m) \end{aligned} \quad (34)$$

for each value of the external Matsubara frequency $i\omega_m$. Finally, analytical continuation to real frequencies $\omega + i0$ is performed using Padé approximants for the first few tens of Matsubara frequencies to obtain the retarded

contact correlator $X^R(\omega)$ in (20), which yields the bulk viscosity via Eq. (21).

At high temperature, the vertex corrections are sub-leading and it suffices to use the bare contact vertex $\delta \Gamma^{-1} = \delta g_0^{-1}$, such that (34) simplifies to

$$\begin{aligned} \chi_{\text{vir}}(\mathbf{k} = 0, i\omega_m) &= X_{\text{vir}}(i\omega_m) \\ &= \frac{m^4}{\beta V} \sum_{\mathbf{q}\epsilon_n} \Gamma(\mathbf{q}, i\epsilon_n) \Gamma(\mathbf{q}, i\epsilon_n + i\omega_m) \end{aligned} \quad (35)$$

in agreement with the first term in Eq. (19). Hence, the virial limit is contained within the LW approach.

In the BEC limit $a \rightarrow 0^+$, the pair propagator has a large gap of order $\epsilon_B \gg \epsilon_F, T$ between the bound state branch and the continuum of dissociated pairs. However, the bound state branch is no longer a δ peak as in Eq. (24) but is broadened due to atom-dimer and dimer-dimer scattering contained within the dressed propagators and the vertex corrections in the LW equations. This broadening gives rise to a finite bound-bound contribution to the bulk viscosity, which should approach the dc bulk viscosity of a weakly repulsive Bose gas as $a \rightarrow 0^+$.

Importance of contact vertex corrections

While in the high-temperature limit the fully dressed contact vertex $\delta \Gamma^{-1}(\mathbf{q}, i\epsilon_n; i\omega_m)$ is close to the bare contact vertex $\delta g_0^{-1} = -m^2$, it is found to be substantially renormalized in the quantum degenerate regime approaching T_c . In particular, at the superfluid phase transition the pair propagator $\Gamma \sim 1/(\xi^{-2} + q^2)$ becomes gapless and gives rise to divergent critical fluctuations as the correlation length $\xi \rightarrow \infty$ diverges. One might expect that the contact correlations (34) would also diverge with a positive power of ξ . However, the contact vertex corrections δM which are included within the Luttinger-Ward approach strongly suppress the static contact vertex at small momenta and result in a scaling form $\delta \Gamma^{-1}(\mathbf{q}, 0; 0) \sim q^2$, which renders the contact correlation less singular when approaching T_c . This is illustrated in Fig. 4, which shows the fully renormalized contact vertex in units of the bare contact vertex δg_0^{-1} : at large momenta $q \gg k_F$ it remains unrenormalized, but is strongly suppressed as $\sim q^2$ for small momenta $\xi^{-1} \ll q \ll k_F$ before it eventually saturates for $q \ll \xi^{-1}$, where ξ depends on the distance from T_c .